good dispersion in water, a specially prepared CNTEC® produced by Kuraray Living Co., Ltd., (Tokyo, Japan) was used as described in Section 2.2.

2.2. Preparation of mixtures and ESR-DMPO method

The measuring mixture consisted of MWCNTs, hydrogen peroxide, ferrous chloride, and 5,5-dimethyl-1-pyrroline-1-oxide (DMPO). Hydrogen peroxide (hydrogen peroxide 30.0–35.5 mass%, Wako Pure Chemical Industries, Ltd., Osaka, Japan) was diluted to 0.1 M with ultrapure water. The 0.1 M solution was diluted to 1 mM with ultrapure water before use. Ferrous chloride (iron (II) chloride tetrahydrate, Wako Pure Chemical Industries, Ltd., Osaka, Japan) was dissolved in ultrapure water to 15.7 mM. This solution was also diluted 100 times before use. Frozen DMPO (Dojindo Laboratories, Kumamoto, Japan) was thawed at room temperature and diluted to 100 mM with ultrapure water. The DMPO solution was prepared each time and disposed within 24 h after preparation. The surfactant for CS-MWCNTs was sodium dodecyl benzensulfonate (SDBS) (Kanto Chemical Co., Inc., Tokyo, Japan) and was diluted to 45.9 mM with ultrapure water.

CNTEC® was made of polyester fibers coated with 12 wt% Nanocyl NC-7000 in dry condition. The weight ratio of the concentration of the surfactant to MWCNTs of CNTEC®, which was specially prepared, was fixed at 26.2:100 in dry condition. In 50 g of ultrapure water, 0.1 g CNTEC fibers were dispersed, which was sonicated for 30 min in a ultrasonic bath. The mixture was filtered with a Whatman filter paper (Whatman 42 with pore size at 2.5 μm) to remove polyester fibers and large agglomerates of MWCNTs. This solution was named as Solution A, which included 0.13 wt% of MWCNTs after drying the solution. Solution A was filtered with a Whatman filter paper (GF/F with pore size 0.7 μm) and then a Milipore filter (MF-Milipore GSWP 09000 m with pore size at 0.22 μm). This solution, named Solution B, included 0.036 wt% of MWCNTs. The procedure gave an advantage to balancing the surfactant interference despite alterations in MWCNT concentration. These solutions were used instead of CS-MWCNTs that were dispersed in the surfactant solution.

In all measurements, the peroxide concentration was in excess.

2.3. Electron spin resonance measurement

All solutions were mixed and measured at room temperature with electron spin resonance (ESR) (JES-FA100, JEOL). The ESR settings were as follows: frequency 9415.404 MHz, power 0.998 mW, field center 335 mT, sweep time 2 min, width ± 5 mT, and modulation frequency 100 kHz. All measurements were conducted within 5 min after mixing all of the solutions. The details were reported in a previous article [26].

ESR spectra were normalized using Mixture B in Table 1 with 0.1 ml CNT solution for all of the CS-MWCNT measurements. With Nanocyl NC-7000, Mixture A in Table 1 without surfactant was used. The ESR measurement results were obtained as relative values to a reference. In the present work, the radical concentration in a reference solution or specified MWCNT mixture was described using the normalized form:

$$\text{Scavenging ratio} = [\text{ESR signal of a sample/ESR signal of a reference}] = [\text{radical concentration of a sample /radical concentration of a reference}]$$

As the ratio is 1 at MWCNT = 0, radical concentration with a change of CNT concentration was expressed as radical concentration ratio to the reference. On the other hand, the radical scavenging rate is described as:

$$\text{Scavenging rate} = \{1 - (\text{Scavenging ratio})\}$$

ESR spectra were normalized using Mixture B in Table 1 with 0.1 ml CNT solution for all of the CS-MWCNT measurements. With Nanocyl NC-7000, Mixture A in Table 1 without surfactant was used. Thus, the scavenging ratio and rate represent the normalized hydroxyl radical concentration relative to the reference and the normalized hydroxyl radical concentration amount scavenged in a solution, respectively. All of the samples were measured at least five times and arithmetically averaged except the lowest and highest values. In the present work, a buffer to control solution pH was not added because the buffer apparently affects the reaction and the reactive components were in the aqueous solution. pH measurement was not conducted during ESR-DMPO measurement because it cannot be physically measured during the ESR spectrum measurements.

3. Results and discussion

3.1. Reaction kinetics hypothesized

According to recent findings, MWCNTs scavenge ROS [23–26]. All of these reports hinted that the reaction occurs at dangling bonds on CNT surfaces and MWCNTs supposedly act as electron donors or, at least, charge is transferred from those dangling bonds to radicals. Petersen et al. reported that SWCNTs also scavenge hydroxyl radicals by electron transfer [27]. Peng et al. found that MWCNTs attached with cadmium sulfide (CdS) were electron acceptors and catalyzed the conversion of water to hydrogen (and inevitably oxygen) in a photoreaction as a simulated photosynthetic reaction, where radical formation and degeneration were implicitly included [28]. This indicates that MWCNTs can be both electron acceptors and donators in redox reactions depending on their relative chemical potentials. If the redox potential is hypothesized for MWCNTs, they may decrease oxidant-induced inflammation of tissues, though the actual condition

Please cite this article in press as: Tsuruoka S et al. Radical scavenging reaction kinetics with multiwalled carbon nanotubes. Carbon (2014), http://dx.doi.org/10.1016/j.carbon.2014.10.009

Table 1 – Solution mixture components for CS-MWCNTs.

Amount of solutions taken (ml)							
Solutions	$FeCl_2$	CNTs in surfactant	DMPO	Surfactant	H_2O_2	Ultrapure water	Total volume
Mixture A	0.4	None	0.4	0.4–0.8	0.4	Balance	2.0
Mixture B	0.4	0–0.4	0.4	Balance	0.4	0.4	2.0

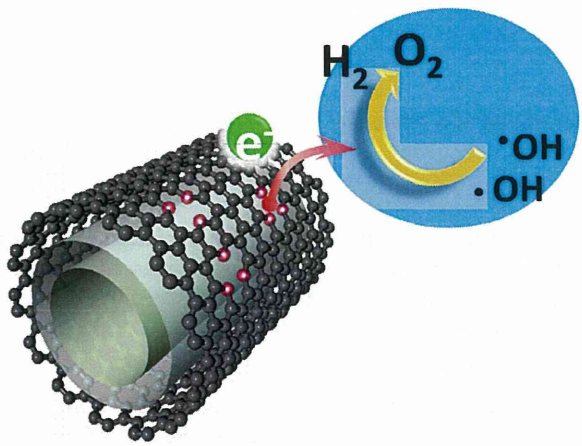

Fig. 2 – A schematic diagram to illustrate hypothesized reaction kinetics of hydroxyl radicals at a reaction site of MWCNTs. For easy visualization of the assumed concept, it is illustrated as if the reaction takes place at a dangling bond. Reaction sites donate electrons to hydroxyl radicals and result in hydrogen and oxygen as denoted in Eq. (6). (A color version of this figure can be viewed online.)

surrounding MWCNTs is complicated. One would be able to stoichiometrically predict oxidant stress once the redox potential of MWCNTs is determined in a reaction system. To conduct and specify CNT behavior in aqueous solution, it is necessary to model it using a simple first-order reaction profile for CNTs as the first step.

We hypothesize the following chemical reaction equations with MWCNTs and hydrogen peroxide (Fig. 2). First, in the light of the fact that a description of the Fenton reaction has not been agreed upon completely, a simple system consisting of hydrogen peroxide and Fe(II) can be written to characterize the present experimental system specifically as follows [29,30]:

$$Fe^{2+} + H_2O_2 \rightarrow Fe^{3+} + HO^- + HO^{\cdot} \quad (1)$$

$$Fe^{3+} + H_2O_2 \rightarrow Fe^{2+} + H^+ + HOO^{\cdot} \quad (2)$$

$$Fe^{3+} + HOO^{\cdot} \rightarrow Fe^{2+} + H^+ + O_2 \quad (3)$$

These equations can be summarized as follows:

$$3H_2O_2 \rightarrow 2H_2O + O_2 + 2HO^{\cdot} \quad (4)$$

According to previous reports [12,20,22–25], it is agreed that CNTs scavenge hydroxyl radicals in an aqueous solution with hydrogen peroxide experimentally. The assumed reaction sites on the CNT surface including dangling bonds are denoted as Dn that acts as if they were single molecules. As long as Eq. (4) is true, a necessary condition to satisfy it with radical scavenging must become an equation as follows:

$$2Dn + 2HO^{\cdot} \rightarrow 2Dn^{+} + H_2 + O_2 \quad (5)$$

Accordingly, Eqs. (4) and (5) give the following equation:

$$3H_2O_2 + 2Dn \rightarrow 2Dn^{+} + 2H_2O + H_2 + 2O_2 \quad (6)$$

Eq. (5) indicates that the reaction sites donate electrons to hydroxyl radicals finitely. This agrees with the assumption of H+ or OH radical generation by electron acceptance on CNTs by Peng et al. [28] In Eq. (6), the reaction rate constant should become "1" if the concentration of Dn is large enough and dominates compared to that of H_2O_2 from Eqs. (S5) to (S6) in the Supplemental. This suggests that this experimental condition must be avoided. Furthermore, the equations predict that the CNT amount, or mole equivalent of the number of reaction sites, is necessarily smaller than that of hydrogen peroxide. Thus, while the mole equivalent of CNTs or reaction sites has not been determined, a concentration ratio of hydrogen peroxide to CNTs should be sought in an experiment.

Eq. (5) requires one to measure the concentrations of hydrogen and oxygen in a scavenging reaction in order to verify the Fenton reactions. However, it is experimentally impossible to measure these concentrations in situ because of the measuring system of the ESR equipment and its measuring cell structure. Fortunately, Eq. (5) is a fictitious reaction to deduce Eq. (6) so that Eq. (5) is regarded as an intermediate reaction. Although the Fenton reaction gives many routes of reaction steps, it can be simplified in such a manner.

3.2. *Influences of chemicals in a reaction system*

Before conducting chemical tests to investigate whether Eq. (6) is appropriate to describe the present chemical reaction, it is necessary to investigate influences by chemicals in an ROS measurement. This has not been pursued previously, because the present approach with chemical kinetics had not been proposed nor systematically explored. In addition, it was reported that chemicals in similar systems significantly affect ESR-DMPO measurement [31]. We conducted a series of tests using CS-MWCNTs (Fig. 1), because they have many edges of graphene that are relatively reactive in comparison with highly crystallized CNTs [26]. Fig. 3a shows that the radical scavenging rate varies with a concentration change of the surfactant without CS-MWCNTs, where Mixture A in Table 1 was used. A reference solution was at 0 mM of the surfactant of Mixture A in Table 1. The results show that hydroxyl radicals are scavenged proportional to a surfactant concentration. Fig. 3a apparently indicates that the surfactant scavenges radicals. Fig. 3b shows the radical scavenging rate

Please cite this article in press as: Tsuruoka S et al. Radical scavenging reaction kinetics with multiwalled carbon nanotubes. Carbon (2014), http://dx.doi.org/10.1016/j.carbon.2014.10.009

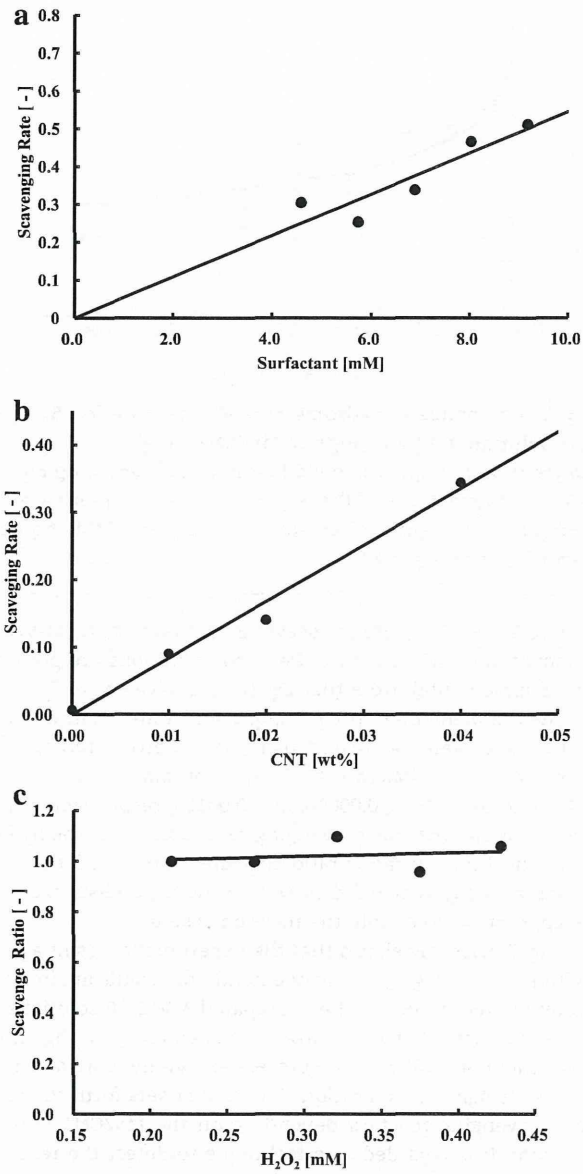

Fig. 3 – Influences of chemical components in the scavenging reaction system. Vertical axis shows the scavenging rate of hydroxyl radicals that were generated by the Fenton reaction with hydrogen peroxide. (a) Influence of surfactant without CS-MWCNTs. The scavenging rate is proportional to surfactant concentration. (b) A scavenging rate change with a change of CS-MWCNT concentration at a fixed surfactant concentration of 0.918 mM. Scavenging rate proportionally corresponds to the MWCNT concentration change. (c) The scavenging ratio with a change of hydrogen peroxide concentration in fixed concentrations of $FeCl_2$ and surfactant in Mixture B without CS-MWCNTs in Table 1. It is apparent that the radical concentration is constant at the measuring time in the solution.

with a concentration change of MWCNTs in a fixed concentration of surfactant at 0.918 mM in a solution, where Mixture B was used in Table 1. Likewise, the reference solution was at 0 wt% of MWCNTs of Mixture B in Table 1. As the scavenging rate of hydroxyl radicals proportionally corresponds to the surfactant concentration according to Fig. 3a, Fig. 3b indicates that the scavenging rate is proportional to the concentration change of CS-MWCNTs at a fixed surfactant concentration, where the surfactant contribution is relatively low. This suggests that the ESR-DMPO method can measure radical concentration changes corresponding to a CS-MWCNT concentration change. However, an intrinsic CS-MWCNT scavenging performance cannot be measured using this method because the respective contributions of CS-MWCNTs and surfactant are not distinguished individually. Fig. 3c demonstrates the scavenging ratio with a change of hydrogen peroxide concentration at a fixed concentration of surfactant without CS-MWCNTs. The scavenging ratio does not change with a change in hydrogen peroxide concentration, which indicates that hydroxyl radical generation depends on the duration of time after mixing these chemicals rather than the hydrogen peroxide concentration under the proposed experimental condition. It is in agreement with the previous literature [29,30]. Therefore, the surfactant is specifically a major influence factor in the present chemical reaction system. It is necessary to minimize the surfactant concentration to determine the intrinsic MWCNT radical scavenging performance.

In our radical scavenging tests with MWCNTs, pH measurements were omitted. On the one hand, there is physical obstruction in which the DMPO adduct has a very short lifetime and the measuring cell cannot be equipped with a pH cell inside due to physical constraints. It did not allow the measurement of pH in situ. On the other hand, the interaction among the buffer chemicals, MWCNTs, and DMPO is complicated and cannot be predicted. The reaction sites on MWCNTs might react with phosphate and DMPO could attach on the CNT surface [32]. It is noted that the pH of the solution mixture just before ESR measurement was approximately 6.5; this was almost equal to that of ultrapure water used. It is regarded that water stabilized pH due to the very low concentration. It would be optimal to estimate or measure the solution pH during ESR-DMPO spectra measurement.

3.3. *Scavenging performance measurements with the minimal amount of surfactant and intrinsic redox potential of MWCNTs*

As mentioned above, because of the influence of surfactant scavenging, performance measurements were conducted using a minimal amount of surfactant with MWCNTs to determine the intrinsic contribution of MWCNTs to radical scavenging. Fig. 4 shows a change in scavenging rate with a change of MWCNT solution volume, where Solution A or B was added into water. This figure clearly shows that the radical scavenging depends on MWCNT concentration. In this procedure, the surfactant concentration in Solutions A and B was identical. Because these solutions were diluted further with ultrapure water and hydrogen peroxide in the measurement, surfactant concentration was two to three digits lower than that of Mixture A or B, which were prepared using a conventional method with surfactant. As the surfactant amount was proportional to the MWCNT concentration which was

Please cite this article in press as: Tsuruoka S et al. Radical scavenging reaction kinetics with multiwalled carbon nanotubes. Carbon (2014), http://dx.doi.org/10.1016/j.carbon.2014.10.009

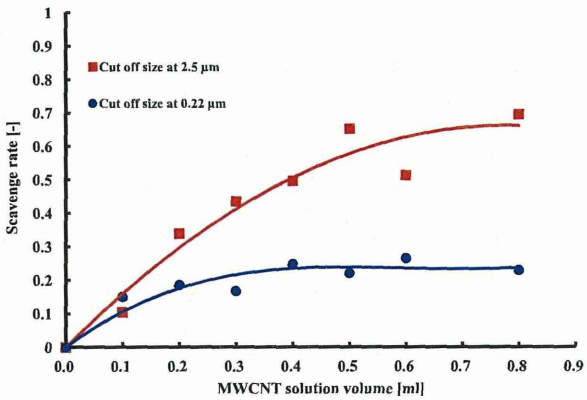

Fig. 4 – Radical scavenging rate with a volume change of MWCNT solutions A and B. Solutions A and B are filtered at 2.5 and 0.22 μm, respectively, to control MWCNT weight concentration. These fitting curves are binominal for Solution A and section three approximations for Solution B, respectively. From these fitting curves, the equilibrium points of Solutions A and B are found to be at 0.78 and 0.38, respectively. (A color version of this figure can be viewed online.)

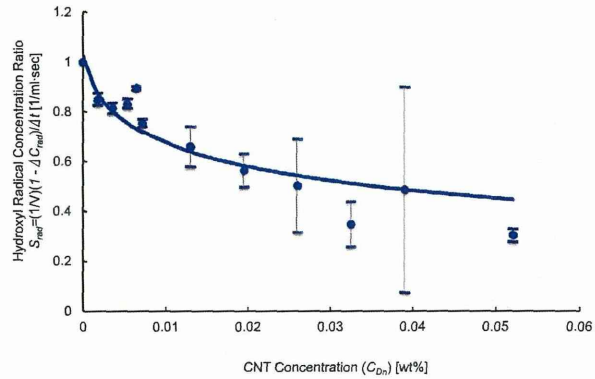

Fig. 5 – A change of hydroxyl radical concentration S_{rad} in the solution with a change of MWCNT weight concentrations C_{Dn}. The solid line is calculated using Eq. (7). Standard deviations of these plots by measurement are indicated with vertical bars. (A color version of this figure can be viewed online.)

low, the influence of the surfactant was believed to be negligible in Solutions A and B according to Fig. 3a. Fig. 4 demonstrates that the maximum of the hydroxyl radical scavenging rate depends on MWCNT concentration and shows their plateau points. This result suggests that the number of reaction sites was significantly different between these solutions.

In comparison with the experimental results discussed in the previous section, the curvature in Fig. 4 is apparently different from that in Fig. 3b. Although it was true that the size distributions of MWCNTs in Solutions A and B were not identical after passing through those filters, the tendency of these curves was alike. The results are consistent with a previous report in which the size difference of particular MWCNTs did not significantly affect the scavenging characteristics though the surface morphological difference did [26]. Another report used MWCNT weight concentration in the horizontal axis instead of volumetric concentration used in Fig. 4. A single smooth line resulted when these results were plotted against each other [31]. From these facts, it is suggested that the scavenging reaction is proportional to the surface area of MWCNTs or the number of reaction sites. Besides, Fig. 4 indicates that the scavenging rate does not increase in a straight line as in Fig. 3a, or the first-order reaction to CNT concentration. Even though peroxide was excessive in quantity, radicals were generated but not so rapidly. Therefore, the scavenging rate exhibits a plateau. It indicates that there is an equilibrium point by an unknown mechanism. However, this is not the target of the present study. Thus, Eq. (5) is an intermediate reaction simply given to derive Eq. (6) with the Fenton reactions.

In Fig. 5, all plots measured with Solutions A and B are summarized together. The solid line is calculated by Eq. (7) as:

$$S_{rad} = -q\ ln|C_{Dn} + s| + q(C_{Dn} + s) + r \tag{7}$$

where S_{rad} and C_{Dn} are the scavenging ratio and the MWCNT concentration in a mixture. Detailed definitions are given in the Supplemental. Note that Eq. (7) is equivalent to Eq. (S8′) in the Supplemental. In Eq. (7), q, r, and s are arbitrary constants and were calculated using the "Solver" function of Microsoft Excel (Microsoft® Excel® for Mac 2011, Version 14.3.9) to be 0.14936, 0.00000, and 0.00105, respectively. Fig. 5 clearly shows that the scavenging reaction ratio or the hydroxyl radical concentration ratio measured agrees with the solid line practically, which indicates that the hypothesis in Eq. (6) is appropriate to denote the reaction system.

Fig. 5 evidently shows that the experimental result agrees with Eq. (7). In Fig. 4, on the one hand, the results are individually plotted based on these prepared MWCNT solutions in order to show CNT concentration dependency. In Fig. 5, on the other hand, all plots are processed together with a change of CNT weight concentration. The former sets forth the radical scavenging reaction depending on the MWCNT surface amount. It is regarded as a technique to detect the reaction rates at very low concentrations of MWCNTs without a change of the other ingredients in the solution. The latter is used to analyze the reaction kinetics. These measurement standard deviations tend to be small at the lower MWCNT concentrations. It is probable that radical scavenging by the surfactant may become significant at higher MWCNT concentrations as the surfactant concentration is proportional to the MWCNT concentration. It is necessary to look for a method to determine the reaction rates of hydroxyl radicals–DMPO and hydroxyl radicals–surfactant to verify the point.

The plateau point is supposed as a pseudo-equilibrium point in this particular reaction system, and may be related to the number of reaction sites of MWCNTs. However, when Eq. (7) is expanded using the Taylor expansion, it is rewritten, if C_{Dn} is large enough, as:

$$S_{rad} = -q\left\{2\left(C_{Dn} + \frac{C_{Dn}^3}{3} + \cdots + \frac{C_{Dn}^{2n+1}}{2n+1} + \cdots\right)\right\} + qC_{Dn} + r$$
$$= -q(C_Dn) + \cdots + \frac{C_{Dn}^{2n+1}}{2n+1} \tag{7′}$$

Please cite this article in press as: Tsuruoka S et al. Radical scavenging reaction kinetics with multiwalled carbon nanotubes. Carbon (2014), http://dx.doi.org/10.1016/j.carbon.2014.10.009

Thus, S_{rad} is to be the infinite number and does not have an equilibrium point at large C_{Dn}, while it has an inflection point. It is considered that Eq. (7) may hold true for a condition at low MWCNT or reaction site concentration having a pseudo-plateau point. It means that the scavenging ratio becomes large at a high MWCNT concentration. At present, as mentioned above, this cannot be practically verified as the higher MWCNT concentration brings a greater influence of surfactant, and consequently the surfactant conceals the intrinsic scavenging activity by MWCNTs. It is necessary to develop a technique to disperse a large amount of MWCNTs at a very low concentration of surfactant. However, the intrinsic behavior of MWCNTs can be sought at very low concentrations of components. Differentiating Eq. (7) and setting to zero, it gives a pseudo-equilibrium point at which a slope of Eq. (7) is horizontal. To solve the equation, $C_{Dn} = s = 0.9985$, and $S_{rad} = q = 0.14936$. This result gives an answer to Eq. (S2); however, it does not specify the pseudo-equilibrium constants of K_1 or K_2, because the actual peroxide concentration in the chemical reaction system is not dynamically determined in the present procedure. It is necessary to seek and develop a measuring method for hydrogen peroxide in the solution in situ and obtain these constants. Even in view of them, Eq. (7) should be applied to the radical scavenging ability of MWCNTs and their bioavailability evaluations. Here, it has to be determined whether the given nano-carbons are to be electron acceptors or donators. Krusic et al. specified that fullerenes were endohedral and electron acceptors [33]. On the other hand, the physical properties of CNTs are significantly different from that of fullerenes, and particularly energy bands and density of state DOS) of CNTs are unique because of the cylindrical structure and chirality [34]. In addition, Ullah et al. proposed a concept of "charge carrier transport mechanism" and discussed that the electron transfer of semiconductive materials is relative [35]. Furthermore, Shi et al. pointed out that CNTs can either donate or accept electrons based on an electron transfer mechanism [36]. As the results of the present work correspond to the previous reports [23–27] and are not inconsistent with those discussions, the assumption of electron donation is reasonable. Thus, Eq. (7) is deemed to be appreciable to those evaluations. Figs. 4 and 5 show that the reaction kinetics between MWCNTs and hydroxyl radicals agree with Eq. (6); that is, MWCNTs donate electrons to those radicals.

Eq. (7) implies that a high concentration of MWCNTs infinitely scavenge hydroxyl radicals, but the scavenging ability by MWCNTs is obviously not proportional to their concentration. Considering these points with the CNT surface structure, the results support our hypothesis semiquantitatively though a pseudo-equilibrium constant is not specified uniquely. One should consider calculating the constant if a CNT chirality gives a particular electron energy distribution and density of state specifically in the case of a thinner diameter [37]. As the electron energy distribution and DOS for thicker-diameter MWCNTs indicate no significant differences [38], a relationship between the redox potential of MWCNTs and chirality has to be clarified with thinner MWCNTs. Furthermore, it is necessary to investigate if Eq. (6) is reversible or kinetically represents an equilibrium condition. Eq. (6), for example, in a biological reaction, predicts that the induction of tissue inflammation after exposure to MWCNTs increases in a long-period test in which the electrons in MWCNTs are depleted, unless the living body can supply electrons to MWCNTs. It has been shown that pulmonary inflammation rapidly increases in the week after exposure to MWCNTs and gradually decreases to a normal condition within a month [39]. The present report suggests that the inflammation decrease may be related to the redox potential. Of interest is whether long-period exposures show a rebound of inflammation. With regard to the electron supply to CNTs, Petersen et al. imply that particular biological reactions give electrons to CNTs [27]. To investigate the biological reaction kinetically, it is necessary to elucidate the Fenton reaction and reactions of biological molecules in the living body. Thus, MWCNTs may have redox potential, while their reactivity as electron acceptors must be proved using an alternative way [40]. Once the redox potential of MWCNTs is determined, MWCNT intrinsic toxicity via ROS can be estimated in tissues chemically using their physicochemical properties and surrounding conditions. Thus, it may be possible that the redox potential of MWCNTs can predict biological responses if the reaction conditions around MWCNTs are determined.

4. Conclusion

A chemical kinetics scheme to explain the hydroxyl radical scavenging mechanism with MWCNTs is proposed and proven by experiments in a simple chemical system with MWCNTs. Theoretical calculations agree with the experimental results. The surfactant was specified as an interfering factor in the present reaction system. Minimizing surfactant concentration allowed demonstration of the intrinsic behavior of MWCNTs in the system. MWCNTs behave as electron donors through their reaction sites, which is a reason why MWCNTs are ROS scavengers. While it is predicted that the surface morphology of MWCNTs can be characterized using chemical reactions on the surface, the present work clearly shows that experimental results agree with chemical kinetics assumed and previous reports. It suggests that this new approach may allow one to estimate toxic reactions based on chemical kinetics using the physicochemical properties of MWCNTs. Although it is necessary to determine the mole equivalent number of MWCNTs to calculate the absolute reaction and equilibrium constants, a model using redox potential and chemical kinetics may predict the intrinsic chemical reactivity of the MWCNT surface and, therefore, be applied to design safer CNT structures.

Acknowledgments

This work is a part of the research program "Development of innovative methodology for safety assessment of industrial nanomaterials" supported by the Ministry of Economy, Trade and Industry (METI) of Japan. ST, KK, and UY were supported by the Exotic Nanocarbon Projects, Japan Regional Innovation Strategy Program by Excellence, Japan Science and Technology Agency (JST). We would like to thank Dr. K. Fujisawa for preparation of the graphic figure for Fig. 1.

Please cite this article in press as: Tsuruoka S et al. Radical scavenging reaction kinetics with multiwalled carbon nanotubes. Carbon (2014), http://dx.doi.org/10.1016/j.carbon.2014.10.009

Appendix A. Supplementary data

Supplementary data associated with this article can be found, in the online version, at http://dx.doi.org/10.1016/j.carbon.2014.10.009.

REFERENCES

[1] Eklund P, Ajayan P, Blackmon R, Hart AJ, Kong J, Prashan B, et al. WTEC panel report on International assessment of research and development of carbon nanotubes manufacturing and applications. World Technology Evaluation Center, Inc.; 2007.
[2] Endo M, Muramatsu H, Hayashi T, Kim YA, Terrones M, Dresselhaus MS. Nature 2005;433:476.
[3] Muramatsu H, Hayashi T, Kim YA, Shimamoto D, Endo M, Meunier V, et al. Small 2009;5:2678–82.
[4] Muramatsu H, Shimamoto D, Hayashi T, Kim YA, Endo M, Terrones M, et al. Adv Mater 2011;23:1761–4.
[5] Fujimori T, Morelos-Gómez A, Zhu Z, Muramatsu H, Futamura R, Urita K, et al. Nat Commun 2013;4. Article number: 2162.
[6] Endo M, Kim YA, Hayashi T, Fukai T, Oshida F, Terrones M, et al. Appl Phys Lett 2002;80:1267–9.
[7] Hayashi T, O'Connor TC, Higashiyama K, Nishi K, Fujisawa K, Muramatsu H, et al. Nanoscale 2013;5:10043–670.
[8] Endo M, Noguchi T, Ito M, Takeuchi K, Hayashi T, Kim YA, et al. Adv Funct Mater 2008;18:3403–9.
[9] Endo M, Takeuchi K, Noguchi T, Asano Y, Fujisawa K, Kim YA, et al. Ind Eng Chem Res 2010;49:9798–802.
[10] Sotowa C, Origi G, Takeuchi M, Nishimura Y, Takeuchi K, Jang IY, et al. ChemSusChem 2008;1:911–5.
[11] Tsuruoka S, Fugetsu B, Khoerunnisa F, Minami D, Takeuchi K, Fujishige M, et al. Mater Express 2013;4:21–9.
[12] Howard J. Current intelligence bulletin 65: occupational exposure to carbon nanotubes and nanofibers. DHHS (NIOSH) Publication; 2013. No. 2013-145.
[13] Tsuruoka S, Cassee FR, Castranova V. Part Fibre Toxicol 2013;10:44.
[14] Donaldson K, Poland CA. Curr Opin Biotechnol 2013;24:724–34.
[15] Guo L, Morris DG, Liu X, Vaslet C, Hurt RH, Kane AB. Chem Mater 2007;19:3472–8.
[16] Ge C, Lao F, Li W, Li Y, Chen C, Qiu Y, et al. Anal Chem 2008;80:9426–34.
[17] Pumera M. Langmuir 2007;23:6453–8.
[18] Pumera M, Miyahara Y. Nanoscale 2009;1:260–5.
[19] Ge C, Li Y, Yin J-J, Liu Y, Wang L, Zhao Y, et al. NPG Asia Mater 2012;4:1–10.
[20] Toh RJ, Ambrosi A, Pumera M. Chem Eur J 2012;18:11593–6.
[21] Liu Y, Zhao Y, Sun B, Chen C. Acc Chem Res 2013;46:702–13.
[22] Liu X, Guo L, Morris D, Kane AB, Hurt H. Carbon 2008;46:489–500.
[23] Fenoglio I, Tomatis M, Lison D, Muller J, Fonseca A, Nagy JB, et al. Free Radical Biol Med 2006;40:227–1233.
[24] Fenoglio I, Greco G, Tomatis M, Muller J, Raymundo-Piñero E, Béguin F, et al. Chem Res Toxicol 2008;21:1690–7.
[25] Murray AR, Kisin E, Leonard SS, Young SH, Kommineni C, Kagan VE, et al. Toxicology 2009;257:161–71.
[26] Tsuruoka S, Takeuchi K, Koyama K, Noguchi T, Endo M, Tristan F, et al. J Phys: Conf Ser 2013;429:01209.
[27] Pertersen EJ, Tu X, Dizdaroglu M, Zheng M, Nelson BC. Small 2013;9(2):205–8.
[28] Peng T, Zeng P, Ke D, Liu X, Zhang X. Energy Fuels 2011;25:2203–10.
[29] Y. Takuma, Bulletin of TIRI 3, Tokyo Institute of Technology [Ph.D. Dissertation] 11719520102, 2008.
[30] Weeks KR, Bruell CJ, Mohanty NR. Soil Sediment Contam 2000;9:331–45.
[31] S. Tsuruoka, H. Matsumoto, K. Takeuchi, K. Koyama, N. Saito, Y. Usui, S. Kobayashi, E. Akiba, D. W. Porter, V. Castranova, F. Cassee, M. Endo, #591 Society of Toxicology 53rd Annual Meeting, Phoenix AZ, 2014.
[32] S. Tsuruoka, K. Takeuchi, K. Koyama, F. Tristan-Lopez, H. Matsumoto, N. Saito, Y. Usui, M. Endo, M. Terrones, D.W. Porter, V. Castranova, #427, Society of Toxicology 52nd Annual Meeting, San Antonio, TX, 2013.
[33] Krusic PJ, Wasserman E, Keizer PN, Morton JR, Preston JF. Science 1991;254:1183–5.
[34] Saito R, Dresselhaus MS, Dresselhaus G. Physical Properties of Carbon Nanotubes. Imperial College Press; 1998.
[35] M. Ullah, A. pivrikas, N. Sedar Sariciftci, H. Sitter, Chapter 8, Charge transport in organic diodes and OFETs: a comparison. In: Sitter H, editor, Small Organic Molecules on Surfaces, Springer Series in Materials Science 173, 2013.
[36] Shi X, Jiang B, Wang J, Yang Y. Carbon 2012;50:1005–13.
[37] Harris PJF. Carbon nanotube science: synthesis, properties and applications. Cambridge University Press; 2009. pp. 146–178.
[38] S. Tsuruoka, Private memorandum to Prof. Natsume at Chiba University in Japan on EED and DOS at large chirality numbers, 2012.
[39] Porter DW, Hubbs AF, Chen BT, McKinney W, Mercer RR, Wolfarth MG, et al. Nanotoxicology 2013;7:1179–94.
[40] Martínez-Morlanes MJ, Castell P, Alonso PJ, Martinez MT, Puértolas JA. Carbon 2012;50:2442–52.

Please cite this article in press as: Tsuruoka S et al. Radical scavenging reaction kinetics with multiwalled carbon nanotubes. Carbon (2014), http://dx.doi.org/10.1016/j.carbon.2014.10.009

Hindawi Publishing Corporation
BioMed Research International
Volume 2015, Article ID 793186, 9 pages
http://dx.doi.org/10.1155/2015/793186

Research Article

Endocytosis of Multiwalled Carbon Nanotubes in Bronchial Epithelial and Mesothelial Cells

Kayo Maruyama,[1] Hisao Haniu,[1,2] Naoto Saito,[1] Yoshikazu Matsuda,[3] Tamotsu Tsukahara,[4] Shinsuke Kobayashi,[2] Manabu Tanaka,[2] Kaoru Aoki,[2] Seiji Takanashi,[2] Masanori Okamoto,[2] and Hiroyuki Kato[2]

[1] *Institute for Biomedical Sciences, Interdisciplinary Cluster for Cutting Edge Research, Shinshu University, 3-1-1 Asahi, Matsumoto, Nagano 390-8621, Japan*
[2] *Department of Orthopaedic Surgery, Shinshu University School of Medicine, 3-1-1 Asahi, Matsumoto, Nagano 390-8621, Japan*
[3] *Clinical Pharmacology Educational Center, Nihon Pharmaceutical University, 10281 Komuro, Ina-machi, Saitama 362-0806, Japan*
[4] *Department of Molecular Pharmacology and Neuroscience, Nagasaki University Graduate School of Biomedical Sciences, 1-14 Bunkyo-machi, Nagasaki 852-8521, Japan*

Correspondence should be addressed to Hisao Haniu; hhaniu@shinshu-u.ac.jp

Received 27 June 2014; Accepted 26 December 2014

Academic Editor: Haseeb A. Khan

Copyright © 2015 Kayo Maruyama et al. This is an open access article distributed under the Creative Commons Attribution License, which permits unrestricted use, distribution, and reproduction in any medium, provided the original work is properly cited.

Bronchial epithelial cells and mesothelial cells are crucial targets for the safety assessment of inhalation of carbon nanotubes (CNTs), which resemble asbestos particles in shape. Intrinsic properties of multiwalled CNTs (MWCNTs) are known to cause potentially hazardous effects on intracellular and extracellular pathways. These interactions alter cellular signaling and affect major cell functions, resulting in cell death, lysosome injury, reactive oxygen species production, apoptosis, and cytokine release. Furthermore, CNTs are emerging as a novel class of autophagy inducers. Thus, in this study, we focused on the mechanisms of MWCNT uptake into the human bronchial epithelial cells (HBECs) and human mesothelial cells (HMCs). We verified that MWCNTs are actively internalized into HBECs and HMCs and were accumulated in the lysosomes of the cells after 24-hour treatment. Next, we determined which endocytosis pathways (clathrin-mediated, caveolae-mediated, and macropinocytosis) were associated with MWCNT internalization by using corresponding endocytosis inhibitors, in two nonphagocytic cell lines derived from bronchial epithelial cells and mesothelioma cells. Clathrin-mediated endocytosis inhibitors significantly suppressed MWCNT uptake, whereas caveolae-mediated endocytosis and macropinocytosis were also found to be involved in MWCNT uptake. Thus, MWCNTs were positively taken up by nonphagocytic cells, and their cytotoxicity was closely related to these three endocytosis pathways.

1. Introduction

Carbon nanotubes (CNTs) were first discovered by Oberlin et al. [1], and they have attracted increasing attention since the end of 20th century. Owing to their unique physical, mechanical, and electronic properties, CNTs serve as valuable reinforcements or enhance the properties and introduce novel functionalities of various materials in a number of fields, including chemistry, electronics, energy, and materials science [2, 3]. The unique properties of CNTs have also garnered considerable attention from the fields of medicine and biology, and they have potential applications as biomaterials for biosensors, drug and vaccine delivery vehicles, and scaffold materials [4–6].

However, the potential adverse effects of CNTs on human health are of great concern, considering their increasing use in composite biomaterials and exploration as innovative solutions for biomedical applications or in nanomedicine as well as the potential workplace exposure [7–9]. CNTs possess asbestos-like morphological characteristics (i.e., a nanoscale size and a high aspect ratio) and persist in the human body for a long time [10–12]. In 2008, Takagi et al. reported that

transgenic mice intraperitoneally injected with MWCNTs exhibited mesothelioma similar to that in mice exposed to asbestos [13]. Subsequently, induction of mesothelioma was also reported after intraperitoneal or intrascrotal injection of CNTs in rodents [14–16]. Moreover, some evidence suggests that CNT causes cancer upon inhalation or intratracheal administration [17–20], although there is no direct evidence that CNTs induce pleural mesothelioma and lung cancer [17, 21–24].

Previous studies have clarified the carcinogenic mechanisms of CNTs in vitro. The number of micronuclei in lung epithelial cells increases upon exposure to MWCNTs, which is indicative of genotoxicity such as chromosomal damage or mitotic spindle disruption [20]. Sargent et al. showed that CNTs induce mitotic spindle disruption that results in errors in chromosome number [8, 25–27]. CNTs must be internalized by cells for such phenomena to occur. We have previously reported that it is important for multiwalled CNTs (MWCNTs) to be internalized for cytotoxic effects to be observed in a human mesothelioma cell line (MESO-1) and a human bronchial epithelial cell line (BEAS-2B) [28–30]. However, the internalization mechanism of CNTs is not well known.

In this study, we demonstrated the mechanism underlying CNT internalization in human primary bronchial epithelial cells and mesothelium cells. Moreover, we also demonstrated the internalization mechanism of CNTs in nonphagocytic cells by using various endocytosis inhibitors.

2. Materials and Methods

2.1. Carbon Nanotubes. MWCNTs manufactured by a chemical vapor deposition method [31] were provided by Hodogaya Chemical (MWNT-7; Tokyo, Japan); their properties have been reported previously [32]. The sterilization conditions were autoclaving at 121°C for 15 min. MWCNTs were vortexed for 1 min in 0.1% gelatin (MediGelatin; Nippi, Tokyo, Japan) or 2% fetal bovine serum (FBS; Life Technologies, Grand Island, NY, USA) in phosphate-buffered saline (PBS) and sonicated for 30 min. MWNT-7 was diluted if required, and a volume of 1/100 was added to the cell culture fluid in the following exposure experiments.

2.2. Endocytosis Inhibitors. The endocytosis inhibitors used were previously described by Yumoto et al. [33]. Phenylarsine oxide, indomethacin, nystatin, and 5-(N-ethyl-N-isopropyl)amiloride were purchased from Sigma-Aldrich (St. Louis, MO, USA). Chlorpromazine was purchased from Nacalai Tesque (Kyoto, Japan). Phenylarsine oxide was dissolved in dimethyl sulfoxide (DMSO) and diluted to 0.2–5 mM. Indomethacin was dissolved in ethanol at 50°C and diluted to 5–100 mM. Nystatin was dissolved in DMSO and diluted to 1–20 mM. 5-(N-Ethyl-N-isopropyl)amiloride was dissolved in DMSO and diluted to 5–80 mM. Chlorpromazine was dissolved in PBS and diluted to 2–50 mM.

2.3. Cell Culture. Normal human bronchial epithelial cells (HBECs) were purchased from Lonza (Walkersville, MD, USA). Normal human mesothelial cells (HMCs) were purchased from Zen-Bio, Inc. (Research Triangle Park, NC, USA). The BEAS-2B human bronchial epithelial cell line was purchased from American Type Culture Collection (Manassas, VA, USA). The ACC-MESO-1 human malignant pleural mesothelioma cell line [34] was purchased from RIKEN (Ibaraki, Japan). HBECs were cultured in bronchial/tracheal epithelial cell serum-free growth medium kit with 0.1 μg/mL retinoic acid (Cell Application, San Diego, CA, USA) and passaged every 4 d, with the medium exchanged every alternate day. HMCs were cultured in mesothelial cell growth medium (Zen-Bio, Inc.) and passaged twice a week. Both types of normal cell were used within 5 passages. BEAS-2B cells were cultured in Ham's nutrient mixture F-12 (Nacalai Tesque) with 10% FBS and passaged twice a week. MESO-1 cells were cultured in RPMI 1640 (Nacalai Tesque) with 10% FBS and passaged twice a week. For each experiment, the cells were seeded at a density of 2×10^5 cells/cm^2 and allowed to adhere for 24 h.

2.4. Cell Viability. The cell viability assay was performed as described previously [35]. We performed an Alamar Blue assay (alamarBlue cell viability reagent; Invitrogen, Carlsbad, CA) according to the manufacturer's instructions. Cells were plated in 96-well plates and incubated for 24 h at 37°C in the culture medium containing MWCNTs in a dispersant or in a control medium containing only dispersant without MWCNTs. Viable cells metabolized the dye, resulting in increased fluorescence detected by excitation/emission at 530/590 nm using a fluorescence multiplate reader (PowerScan 4; DS Pharma Biomedical, Osaka, Japan). Cell viability was calculated as follows: percent cytotoxicity = 100 × experimental value/control value. The test media were assayed six times for each treatment condition.

2.5. Imaging of MWNT-7 Uptake by Fluorescence Microscopy. Cells were cultured on ibiTreat μ-Slide (ibidi GmbH, Martinsried, Germany) for snapshot imaging and ibiTreat μ-dish for time-lapse imaging for 24 h in a 5% CO_2 incubator. The cells were prestained with bisbenzimide H33342 fluorochrome trihydrochloride (H33342, 1 μg/mL; Nacalai) and CytoPainter Lysosomal Staining Kit (Abcam, Tokyo, Japan) for 2 h. Then, the cells were washed once and exposed to MWNT-7 (10 μg/mL). MWNT-7 uptake was snapshot-imaged at 2, 6, and 24 h, and time-lapse imaging was performed at 10 min intervals for 24 h by using differential interference contrast (DIC) and fluorescence imaging by fluorescence microscopy with cell culture equipment (AxioObserver Z1, Zeiss, Jena, Germany) using a 40x objective.

2.6. Assessment of MWNT-7 Uptake by Flow Cytometry. Cells were cultured on a 12-well plate for 24 h in a 5% CO_2 incubator. Endocytosis inhibitors were pretreated 15 min before CNT exposure. Then, the cells were exposed to MWNT-7 (10 μg/mL) and incubated for 2 h. The evaluation of cellular uptake for MWNT-7 followed the method reported that we reported previously [28]. In brief, the cells treated with or without MWNT-7 were washed twice and trypsinized.

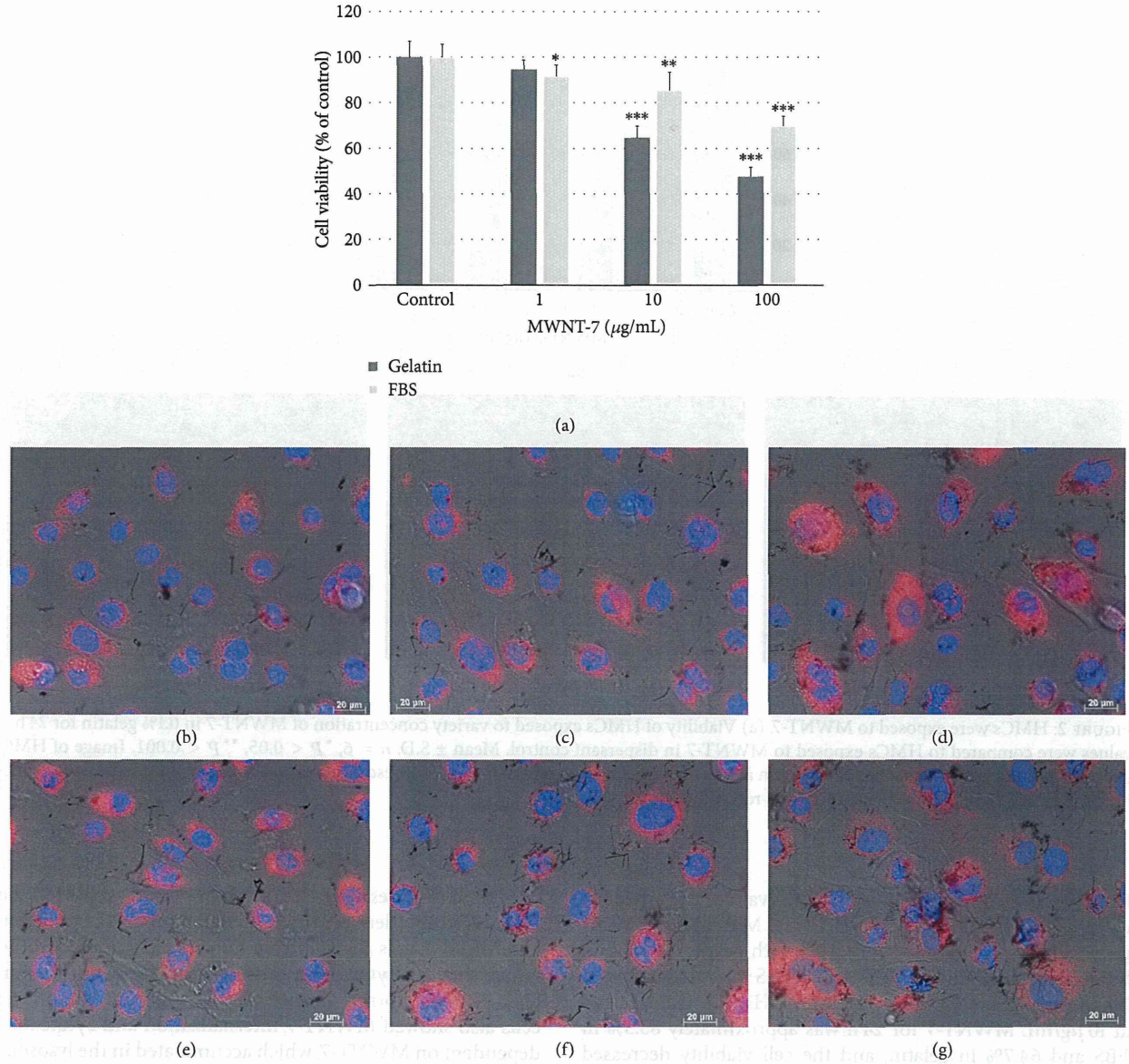

FIGURE 1: HBECs were exposed to MWNT-7. (a) Viability of HBECs exposed to various concentrations of MWNT-7 in 0.1% gelatin or 2% FBS for 24 h. HMCs were compared with HBECs exposed to MWNT-7 in each type of dispersant and to the control. Mean ± SD. $n = 6$, $^{*}P < 0.05$, $^{**}P < 0.01$, and $^{***}P < 0.001$. Image of HBECs exposed to 10 μg/mL MWNT-7 in 0.1% gelatin at 2 h (b), 6 h (c), and 24 h (d) and in 2% FBS at 2 h (e), 6 h (f), and 24 h (g). DIC and fluorescence images were merged. Nuclei were stained blue with H33342 and lysosomes were stained red with CytoPainter.

The cells suspended in PBS containing 10% FBS were filtered through a nylon mesh. Then, the cells were assayed for side scatter (SSC) by light scattering analysis using a flow cytometer (FCM; FACSCalibur, Becton Dickinson, San Jose, CA, USA). The SSC ratio was calculated by dividing the MWNT-7 value with the control value.

2.7. Statistical Analysis. Data are presented as the mean ± standard deviation (SD). Statistical significance was determined by analysis of variance (ANOVA) followed by Student's t-test, and $P < 0.05$ was considered to be significant.

3. Results and Discussion

3.1. Cellular Uptake by HBECs and HMCs. First, we determined whether CNTs could be internalized in normal human bronchial epithelial and mesothelial cells, for which potential carcinogenicity of CNTs is of concern. Although we had already shown that human mesothelioma cells and commercialized normal HBECs from Cell Application internalized CNTs [28, 32, 36], Nagai et al. reported that normal human primary cultured mesothelium cells did not internalize CNTs [16]. We used HBECs purchased from a different company

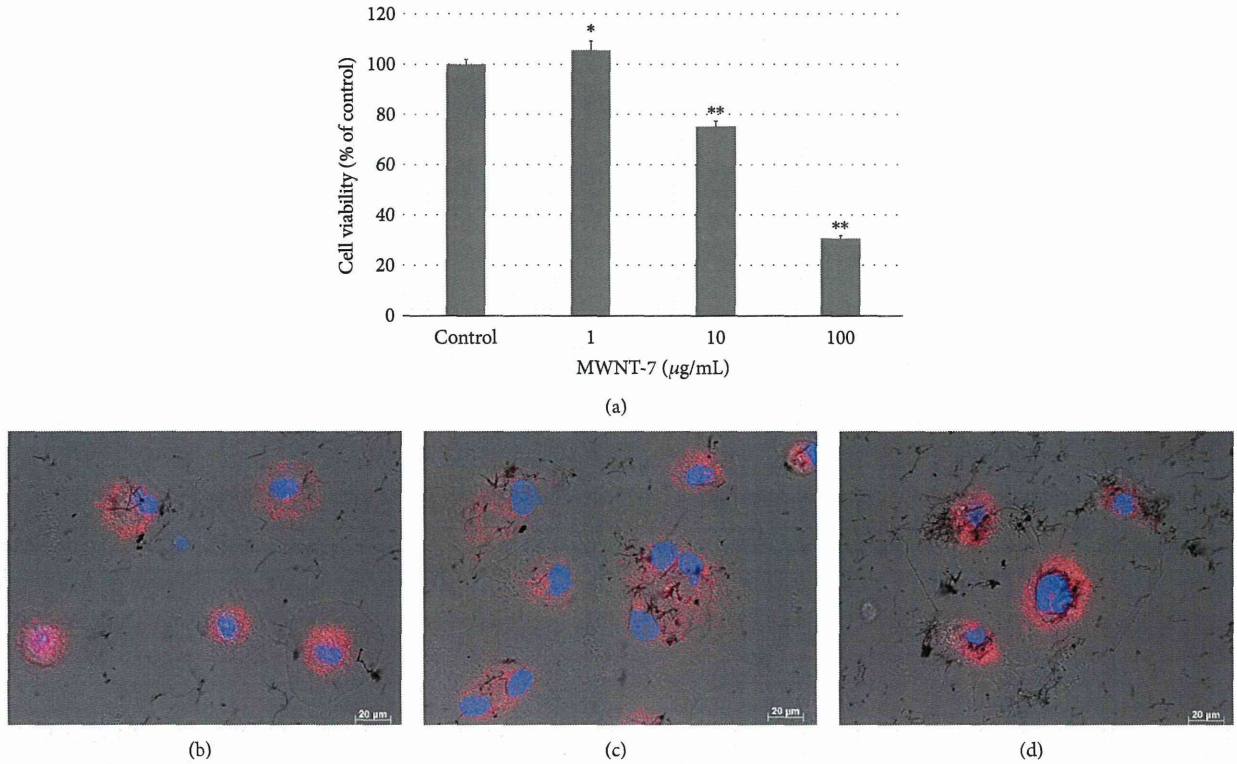

FIGURE 2: HMCs were exposed to MWNT-7. (a) Viability of HMCs exposed to variety concentration of MWNT-7 in 0.1% gelatin for 24 h. P values were compared to HMCs exposed to MWNT-7 in dispersant control. Mean ± S.D. $n = 6$, $^{*}P < 0.05$, $^{**}P < 0.001$. Image of HMCs exposed to 10 μg/mL MWNT-7 in 0.1% gelatin at 2 h (b), 6 h (c), and 24 h (d). DIC and fluorescence images were merged. Nuclei were stained blue with H33342 and lysosome were stained red with CytoPainter.

from that used in the previous paper to evaluate the influence of supplier on cellular uptake of CNTs. Moreover, we compared FBS as a dispersant for CNTs with gelatin in HBECs because the dispersion of CNTs by 2% FBS was recommended by the ENPRA [37]. The viability of HBECs from Lonza at 10 μg/mL MWNT-7 for 24 h was approximately 85.5% in FBS and 64.7% in gelatin, and the cell viability decreased at higher concentrations (100 μg/mL) in both dispersants in a concentration-dependent manner (69.9% versus 47.7%; Figure 1(a)). We observed cells dyed with fluorescence to determine whether CNTs were internalized in the cells. The visualized cells began to internalize MWNT-7 dispersed in not only gelatin but also FBS within 2 h in some cells, and uptake of MWNT-7 was observed in most cells within 6 h (Figures 1(b), 1(c), 1(e), and 1(f)). At 24 h, MWNT-7 appeared to accumulate in lysosomes (Figures 1(d) and 1(g)). Because the purpose of this paper was to elucidate the mechanisms underlying the endocytosis of CNTs, the CNTs used in subsequent experiments were dispersed with gelatin to prevent the influence of unknown factors.

Although the viability of HMCs exposed to MWNT-7 dispersed in gelatin decreased in a concentration-dependent manner (Figure 2(a)) the cell viability was still higher than that of HBECs. HMCs also began to internalize MWNT-7 within 2 h, and the internalization of MWNT-7 increased over time (Figures 2(b)–2(d)). We previously reported that BEAS-2B cells derived from human bronchial epithelium and MESO-1 cells derived from human malignant mesothelioma showed cytotoxicity arising from lysosomal injury [35]. Human normal bronchial epithelial and mesothelial cells also showed MWNT-7 internalization and cytotoxicity dependent on MWNT-7, which accumulated in the lysosome in excessive concentrations. Although Nagai et al. found that human primary mesothelium cells exposed to MWCNTs did not internalize the MWCNTs based on the SSC ratio, transmission electron microscopy, confocal microscopy, and time-lapse microscopy, they evaluated the results at 3 h after exposure to the materials [16]. We speculate that these results were obtained because it is difficult for CNTs to sink in the solution owing to their very light weight. In fact, our results showed that uptake of MWNT-7 observed by DIC increased over time, and only a few cells internalized MWNT-7 in 2 h. It has also been reported that the quantity of CNTs that undergo cellular uptake increases until approximately 12 h [38]. Moreover, although previous studies have evaluated the uptake of CNTs in comparison with asbestos, such a comparison under the same conditions is not effective because cellular uptake of different materials depends on their physicochemical properties. Another study showed that MWCNT exerted adverse effects without CNT uptake in a human mesothelial cell line